Published OnlineFirst February 22, 2008; DOI: 10.1158/1541-7786.MCR-07-2028

Distinct Functions of Natural ADAM-15 Cytoplasmic Domain Variants in Human Mammary Carcinoma

Julia L. Zhong,[1] Zaruhi Poghosyan,[2] Caroline J. Pennington,[1] Xanthe Scott,[1] Madeleine M. Handsley,[1] Alba Warn,[1] Jelena Gavrilovic,[1] Katja Honert,[3] Achim Krüger,[3] Paul N. Span,[4] Fred C.G.J. Sweep,[4] and Dylan R. Edwards[1]

[1]Biomedical Research Centre, School of Biological Sciences, University of East Anglia, Norwich, United Kingdom; [2]Department of Pathology, School of Medicine, Cardiff University, Cardiff, United Kingdom; [3]Institut für Experimentelle Onkologie und Therapieforschung, Klinikum rechts der Isar der Technischen Universität München, Munich, Germany; and [4]Department of Chemical Endocrinology, Radboud University Nijmegen Medical Centre, Nijmegen, the Netherlands

Abstract

Adamalysins [a disintegrin and metalloproteinase (ADAM)] are a family of cell surface transmembrane proteins that have broad biological functions encompassing proteolysis, adhesion, and cell signal regulation. We previously showed that the cytoplasmic domain of ADAM-15 interacts with Src family protein tyrosine kinases and the adaptor protein growth factor receptor binding protein 2 (Grb2). In the present study, we have cloned and characterized four alternatively spliced forms of ADAM-15, which differ only in their cytoplasmic domains. We show that the four ADAM-15 variants were differentially expressed in human mammary carcinoma tissues compared with normal breast. The expression of the individual isoforms did not correlate with age, menopausal status, tumor size or grade, nodal status, Nottingham Prognostic Index, or steroid hormone receptor status. However, higher levels of two isoforms (ADAM-15A and ADAM-5B) were associated with poorer relapse-free survival in node-negative patients, whereas elevated ADAM-15C correlated with better relapse-free survival in node-positive, but not in node-negative, patients. The expression of ADAM-15A and ADAM-15B variants in MDA-MB-435 cells had differential effects on cell morphology, with adhesion, migration, and invasion enhanced by expression of ADAM-15A, whereas ADAM-15B led to reduced adhesion. Using glutathione *S*-transferase pull-down assays, we showed that the cytoplasmic domains of ADAM-15A, ADAM-15B, and ADAM-15C show equivalent abilities to interact with extracellular signal-regulated kinase and the adaptor molecules Grb2 and Tks5/Fish, but associate in an isoform-specific fashion with Nck and the Src and Brk tyrosine kinases. These data indicate that selective expression of ADAM-15 variants in breast cancers could play an important role in determining tumor aggressiveness by interplay with intracellular signaling pathways. (Mol Cancer Res 2008;6(3):383–94)

Introduction

ADAMs (*a d*isintegrin *a*nd *m*etalloproteinases) are membrane-anchored glycoproteins with broad biological functions, including proteolysis, cell adhesion, cell fusion, and intracellular signaling (1, 2). They are multidomain proteins consisting of proproteinase, metalloproteinase, disintegrin, cysteine-rich, epidermal growth factor–like, and cytoplasmic domains, with structural similarity to snake venom reprolysins (ref. 3; see Fig. 1A). To date, 34 ADAM proteins have been identified in different species and the human family contains 23 members. Approximately half have a consensus metalloproteinase catalytic sequence, rendering them proteolytically active, whereas the remainder likely have roles in cell adhesion. Several ADAM family members have been found to release cytokines, growth factors, receptors, adhesion molecules, and other membrane proteins from the cell surface, a process termed ectodomain shedding (1).

ADAM proteins are able to interact with integrins via their disintegrin/cysteine–rich domains. Human ADAM-15 is the only member of the ADAM family with the integrin-binding motif Arg-Gly-Asp (RGD) in its disintegrin domain (4). It binds to $\alpha_v\beta_3$ in monocyte-like U937 and melanoma cells and to $\alpha_5\beta_1$ in T-lymphocyte MOLT cells in an RGD-dependent manner (5, 6) and also interacts with $\alpha_9\beta_1$ in an RGD-independent manner (7), suggesting that ADAM-15 may play a role in cell-to-cell interactions and cell adhesion. The metalloproteinase domain of ADAM-15 has the potential for catalytic activity but its physiologic substrates are as yet undefined, although it was recently shown to cleave and activate heparin-binding epidermal growth factor in mammary cancer cells in response to thrombin (8). Its interactions with integrins and its potential

Received 9/11/07; revised 11/19/07; accepted 11/21/07.
Grant support: Wellcome Trust, the Big C Appeal and the EU Framework Programme 6 Cancerdegradome Project LSHC-CT-2003-503297, and British Heart Foundation studentship FS/03/039/15443.
The costs of publication of this article were defrayed in part by the payment of page charges. This article must therefore be hereby marked *advertisement* in accordance with 18 U.S.C. Section 1734 solely to indicate this fact.
Note: J.L. Zhong and Z. Poghosyan contributed equally to this work.
Requests for reprints: Dylan R. Edwards, Biomedical Research Centre, School of Biological Sciences, University of East Anglia, Norwich Research Park, Norwich NR4 7TJ, United Kingdom. Phone: 44-1603-592184; Fax: 44-1603-592250. E-mail: Dylan.edwards@uea.ac.uk
Copyright © 2008 American Association for Cancer Research.
doi:10.1158/1541-7786.MCR-07-2028

Downloaded from mcr.aacrjournals.org on September 22, 2021. © 2008 American Association for Cancer Research.

Published OnlineFirst February 22, 2008; DOI: 10.1158/1541-7786.MCR-07-2028

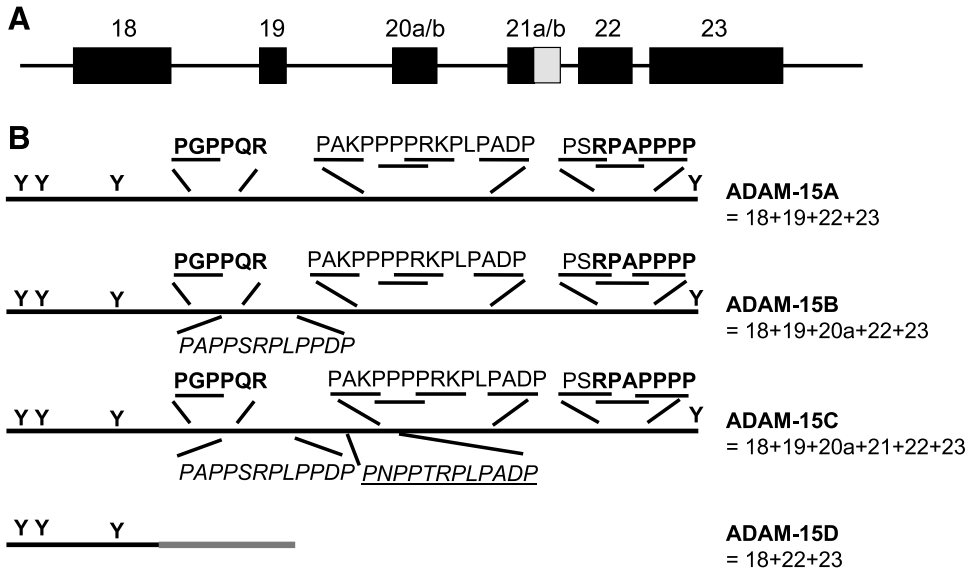

FIGURE 1. Domain organization of ADAM-15 and the sequence differences of the splice variants. **A.** Schematic of the exon organization of the portion of *ADAM15* encompassing the cytoplasmic domain. Exons are shown as numbered black boxes. Exon 20a and 20b differ by one amino acid due to the presence of a tandem NAGNAG splice acceptor sequence (29); exons 21a and 21b differ in their use of the 3′ splice site, as shown by a gray box for the longer exon 21b (29). **B.** Schematic representation of the cytoplasmic domains of the ADAM-15A, ADAM-15B, ADAM-15C, and ADAM-15D variants, and the exons from which they are derived. PXXP motifs are underlined. Class I (R*XX*P*XX*P) and class II (P*XX*P*X*R) ligands for Src family PTK are in boldface type. The National Center for Biotechnology Information protein database entries for these proteins are as follows: ADAM-15A (the original ADAM-15): NP_003806 (814 amino acids); ADAM-15B: NP_997077, with a 75-bp insert, contains one additional proline-rich insert (*italic*); ADAM-15C: NP_997080, with an additional 72-bp insert, contains an additional proline-rich insert (*italic with a line below*); ADAM-15D: NP_997074, the shortest ADAM-15, which introduces a frameshift upstream of the proline-rich regions, which results in insertion of a premature termination codon.

proteolytic functions suggest that as has been described for ADAM-8 and ADAM-12, ADAM-15 could have a significant effect on pathologic processes associated with cancer progression such as tumor cell invasion, migration, and metastasis (9, 10).

The transmembrane ADAM proteins differ in their cytoplasmic domains, with several of them, such as ADAM-9, ADAM-10, ADAM-12, ADAM-15, ADAM-17, and ADAM-22 (11, 12), containing proline-rich regions and tyrosine residues that provide opportunities for interactions with Src homology 3 (SH3) and SH2 domain-containing intracellular proteins such as Src, growth factor receptor binding protein 2 (Grb2), p85 (the regulatory subunit of phosphatidylinositol 3-kinase), MAD2, endophilin I, SH3PX1, and Fish (13-17). We have previously shown the interactions of the ADAM-15 cytoplasmic domain with the Src family protein tyrosine kinases (Lck and Hck), MAD, and adaptor protein Grb2 in hematopoietic cell types (18). Thus, via its cytoplasmic domain, ADAM-15 may be involved in regulating cellular signaling pathways that exert diverse effects on cellular organization and function.

Expression of ADAM-15 has been seen in a broad range of tissues (4), with high levels in vascular cells, the endocardium, bone, and some regions of the brain (19); *Adam15*-deficient mice revealed no major defects during development but have reduced tumor angiogenesis (19), whereas aging *Adam15*-deficient adult mice exhibited accelerated development of osteoarthritic lesions compared with wild-type littermates (20). Altered expression of ADAM-15 has also been seen in tissues associated with inflammation, including osteoarthritic cartilage, rheumatoid synovium, fibrillating human atria, and human papillomavirus–infected gastric mucosa (reviewed ref. 11). Further, elevated ADAM-15 expression has been reported in cell lines from hematologic malignancies; in ovarian, gastric, breast, prostate, and lung cancers and cell lines; and in brain tumors (21-26). The *ADAM15* gene is localized to chromosome band 1q21.3, a region that is amplified in several types of cancers (27, 28). The 23 exons of *ADAM15* display complex patterns of alternative splicing, with a recent study documenting 13 variant forms (29), all of which arise from differential use of exons 18 to 23 that encode the cytoplasmic domain.

In the present work, we have characterized four cytoplasmic domain variants of ADAM-15. We used real-time reverse transcription-PCR to quantify the mRNA levels of all four isoforms in two cohorts of human breast cancer patients, and the correlation between their expression levels and patient survival was investigated. Differential association with patient survival was apparent, with ADAM-15B in particular being strongly linked with poor survival in node-negative patients. Moreover, when overexpressed in MDA-MB-435 cells, ADAM-15A and ADAM-15B isoforms differentially affected cell adhesion and invasiveness. The three ADAM-15 variant cytoplasmic domains that contain proline-rich motifs also showed differential abilities to interact with components of the intracellular signaling apparatus. These data indicate that overexpression of specific ADAM-15 isoforms in breast tumors is linked with clinical outcome, and in particular that ADAM-15B, which has the broadest repertoire of interaction partners, is associated with malignant tumor behavior.

Downloaded from mcr.aacrjournals.org on September 22, 2021. © 2008 American Association for Cancer Research.

Published OnlineFirst February 22, 2008; DOI: 10.1158/1541-7786.MCR-07-2028

Results

Expression of Variant ADAM15 *Isoforms in Breast Cancer and the Relationship with Patient Survival*

We have cloned four variant forms of ADAM-15 (ADAM-15A, ADAM-15B, ADAM-15C, and ADAM-15D), which differ in the sequence of their cytoplasmic domains (Fig. 1). Examination of the genomic sequence of *ADAM15* confirms that all four isoforms are derived by alternative splicing involving exons 18 to 23 (Fig. 1A; ref. 29). The shortest isoform, ADAM-15D, arises due to omission of exons 19 to 21, which causes a reading frame shift in exons 22 and 23 compared with the other three isoforms; this isoform corresponds to variant 1 in Genbank (NM_207191). It thus lacks proline-rich modules and has a distinct sequence of 37 amino acids (shown in gray in the schematic) before the stop codon. The ADAM-15A, ADAM-15B, and ADAM-15C variants all include proline-rich motifs, with exons 19 and 20 introducing additional modules into the core cytoplasmic domain found in the A isoform. The ADAM-15A isoform corresponds to the sequence of the cDNA clone reported originally (4) and is equivalent to Genbank variant 2 (NM_003815); this was also the form of ADAM-15 that was used in our previous work (18). ADAM-15B is Genbank variant 3 (NM_207194); ADAM-15C is Genbank variant 5 (NM_207196). Equivalent isoforms have been observed in the analysis done by Ortiz et al. (25). The ADAM-15D isoform was also observed in studies on human intestinal epithelial cells (30), and the ADAM-15A, ADAM-15B, and ADAM-15C variants were observed in hematopoietic cell types (31). A recent study documented 13 splice variants involving the ADAM-15 cytoplasmic domain (29), which result both from different exon usage and alternative splice sequences in two exons (exons 20 and 21). Thus, there is a complex pattern of exon usage in this gene, but a key point is that this is restricted to the cytoplasmic domain as the extracellular regions are identical in all variants.

We initially analyzed the expression of *ADAM15* in tissues from a small cohort of 48 breast cancer patients, along with 10 normal mammary samples (32). Real-time reverse transcription-PCR expression analysis of total ADAM-15 using a primer-probe set that corresponds to the metalloproteinase domain (which therefore detects all isoforms) did not detect any differences between normal and tumor tissues (data not shown). Subsequently, we designed isoform-specific probes, and the data for ADAM-15A, ADAM-15B, ADAM-15C, and ADAM-15D are shown in Fig. 2. There were no significant changes in the mRNA levels of ADAM-15A and ADAM-15D, but levels from ADAM-15B and ADAM-15C isoforms were significantly higher in breast cancer tissue compared with normal breast. ADAM-15D is expressed at the lowest level ($C_t > 35$), and hence will not be considered further here. However, we carried out further analysis of the expression of the three major isoforms ADAM-15A, ADAM-15B, and ADAM-15C in a larger cohort of 229 breast cancer patients with an extensive (up to 15 years) follow-up period (32, 33). The expression of the individual isoforms did not correlate with age, menopausal status, tumor size or grade, nodal status, Nottingham Prognostic Index, or steroid hormone receptor status (Table 1). Cox regression analysis was carried out to evaluate relationships of the mRNA expression with relapse-free survival (Table 2). In the whole patient group, no association was found between ADAM-15A or ADAM-15B mRNA levels (as entered as log-normalized continuous variables in a Cox regression survival analysis) and relapse-free survival. Subgroup analyses, however, revealed that both ADAM-15A (hazard ratio, 2.095; 95% confidence interval, 1.048-4.191; $P = 0.036$) and ADAM-15B (hazard ratio, 2.923; 95% confidence interval, 1.451-5.888; $P = 0.003$) were associated with a poor survival in the patients with node-negative disease. Conversely, high ADAM-15C expression levels were found in patients with node-positive disease and a good prognosis (hazard ratio, 0.703; 95% confidence interval, 0.503-0.984; $P = 0.040$). These data were confirmed and visualized in Kaplan-Meier analyses as shown in Fig. 3 after dichotomization of the patient groups by the median expression levels.

Taken together, these data show that ADAM-15 isoforms are differentially expressed in breast cancer tissue and that the particular combination of ADAM-15 isoforms has an effect on disease course.

Overexpression of ADAM15 *Variants in Transfected MDA-MB-435 Cell Lines*

In further analyses, we investigated molecular mechanisms underlying these observations by generating stable cell clones of the MDA-MB-435 cell line that has moderate endogenous ADAM-15 expression. Stable transfections of MDA-MB-435 cells were carried out with full-length human ADAM-15A and ADAM-15B in the pcDNA4-V5-His vector, resulting in proteins that carried the COOH-terminal V5-His tags. No stable transfectants of ADAM-15C were generated, either in MDA-MB-435 or in MCF-7 cells (data not shown). Multiple independent clones were isolated for cells transfected with either empty vector or ADAM-15A and ADAM-15B expression constructs, and Fig. 4A shows that levels of expression of two ADAM-15 variant clones chosen for further analysis were comparable and resulted in an ~2- to 4-fold increased level compared with that of the endogenous ADAM-15. Immunostaining with anti-V5 revealed membrane-associated and intracellular immunoreactivity for both isoforms (data not shown). All of the clones exhibited similar levels of vinculin; extracellular signal-regulated kinase (ERK) 1/2; and phosphorylated (P)-ERK1/2, focal adhesion kinase (FAK), Src, and P-Src expression (data not shown), which did not differ among the variants. There were also no apparent differences in the growth rates or levels of apoptosis in ADAM-15–transfected cells compared with vector controls or parental MDA-MB-435 cells (data not shown).

We observed consistent differences between ADAM-15A, ADAM-15B, and vector-transfected cells in terms of cytoskeletal architecture. Representative images of sparsely grown cells immunostained for FAK and the actin cytoskeleton stained with rhodamine-phalloidin are shown in Fig. 4B. The morphologic changes observed were present in the majority of cells. The vector control transfectants resembled the parental MDA-MB-435 cells (data not shown), with cells well spread and prominent actin stress fibers apparent, as well as cortical actin. In contrast, ADAM-15B–expressing cells were less well spread, appear smaller (Fig. 4A), and with stronger cortical actin staining and fewer and shorter actin fibers. The

Downloaded from mcr.aacrjournals.org on September 22, 2021. © 2008 American Association for Cancer Research.

Published OnlineFirst February 22, 2008; DOI: 10.1158/1541-7786.MCR-07-2028

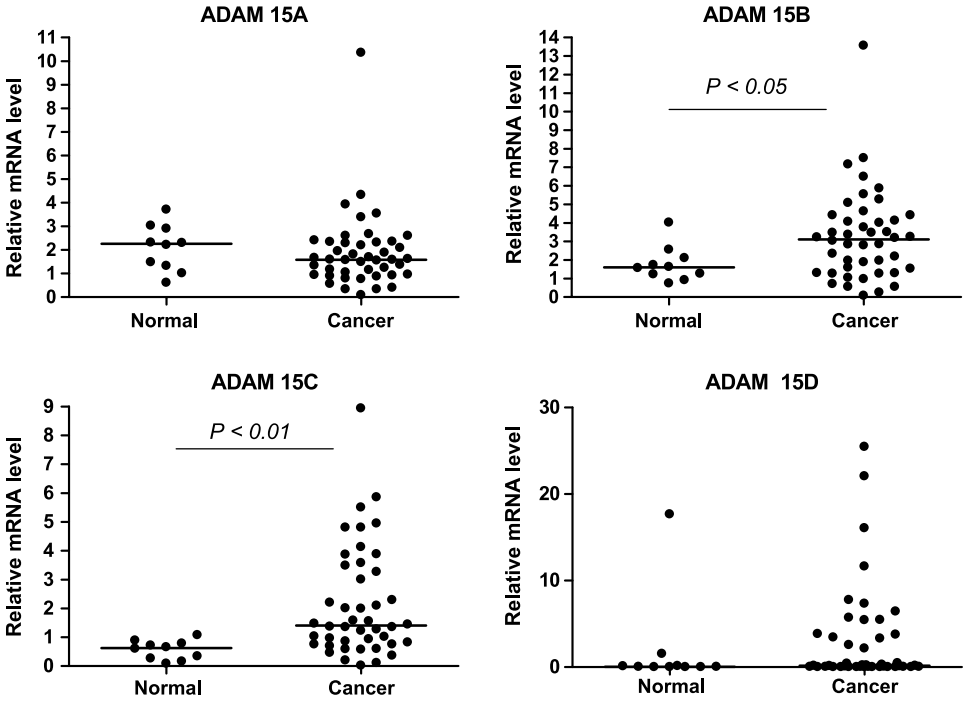

FIGURE 2. Levels of mRNA expression of *ADAM15* isoforms in breast cancer tissues. Expression of ADAM-15A, ADAM-15B, ADAM-15C, and ADAM-15D isoforms was quantified by TaqMan real-time reverse transcription-PCR in 48 breast cancer tissues compared with 10 control normal mammary tissues. Points, mean; bars, SE. Significance was determined by *t* test.

ADAM-15A–transfected cells resembled vector controls in being well spread. FAK showed the typical discrete, short clusters of focal adhesion complex staining, which was enriched at both the central region and the periphery of cells, coincident with the F-actin at focal adhesion sites (Fig. 4B, *bottom*). However, FAK staining in ADAM-15B–expressing cells was less and was more condensed, although the level of FAK and P-FAK (not shown) did not show any difference by

Table 1. Categorical Distributions of Baseline Characteristics in All Patients and Associations with ADAM-15 Isoform Expression Levels

Characteristics	ADAM-15A*			ADAM-15B*			ADAM-15C		
	<Median	>Median	*P* †	<Median	>Median	*P* †	<Median	>Median	*P* †
Age (y)			0.148			0.664			0.991
≤50	31 (59)	22 (41)		28 (53)	25 (47)		26 (49)	27 (51)	
>50	83 (47)	93 (53)		87 (49)	89 (51)		86 (49)	89 (51)	
Menopausal status			0.210			0.239			0.881
Pre	33 (57)	25 (43)		33 (57)	25 (43)		28 (48)	30 (52)	
Post	81 (47)	90 (53)		82 (48)	89 (52)		84 (49)	86 (51)	
Tumor size			0.093			0.608			0.402
pT_1	29 (47)	33 (53)		31 (50)	31 (50)		26 (42)	36 (58)	
pT_2	62 (47)	71 (53)		64 (48)	69 (52)		67 (51)	65 (49)	
pT_{3+4}	21 (68)	10 (32)		18 (58)	13 (42)		17 (55)	14 (45)	
Histologic grade			0.828			0.174			0.196
1/2	39 (49)	41 (53)		46 (58)	34 (42)		39 (49)	41 (51)	
3	41 (53)	37 (47)		39 (50)	39 (50)		33 (42)	45 (58)	
No. involved lymph nodes			0.956			0.194			0.599
0	46 (49)	49 (52)		45 (47)	50 (53)		42 (44)	53 (56)	
1-3	35 (51)	34 (49)		41 (59)	28 (41)		32 (47)	36 (53)	
≥4	20 (49)	21 (51)		18 (44)	23 (56)		22 (54)	19 (46)	
NPI			0.325			0.174			0.977
1	3 (43)	4 (57)		5 (71)	2 (29)		3 (43)	4 (57)	
2	42 (53)	38 (47)		51 (64)	29 (36)		33 (41)	47 (59)	
3	17 (39)	27 (61)		21 (48)	23 (52)		19 (43)	25 (57)	
ER (fmol/mg protein)			0.743			0.123			0.669
<10	38 (49)	40 (51)		34 (44)	44 (56)		39 (51)	38 (49)	
≥10	76 (51)	73 (49)		81 (54)	68 (46)		71 (48)	78 (52)	
PgR (fmol/mg protein)			0.892			0.808			0.174
<10	46 (51)	45 (49)		45 (49)	46 (51)		39 (43)	51 (57)	
≥10	68 (50)	69 (50)		70 (51)	67 (49)		72 (53)	65 (47)	

Abbreviations: NPI, Nottingham Prognostic Index; ER, estrogen receptor; PgR, progesterone receptor.
*Number (percentage). Due to missing values, numbers do not always add up to 229.
†Pearson χ^2.

Downloaded from mcr.aacrjournals.org on September 22, 2021. © 2008 American Association for Cancer Research.

Published OnlineFirst February 22, 2008; DOI: 10.1158/1541-7786.MCR-07-2028

Table 2. Cox Regression Survival Analyses for Total ADAM-15A, ADAM-15B, and ADAM-15C Isoforms

	n	ADAM-15A		ADAM-15B		ADAM-15C	
		HR (95% CI)	*P*	HR (95% CI)	*P*	HR (95% CI)	*P*
All	205	1.168 (0.758-1.799)	0.481	1.348 (0.890-2.040)	0.158	0.775 (0.594-1.011)	0.061
Node-neg	95	2.095 (1.048-4.191)	0.036	2.923 (1.451-5.888)	0.003	1.113 (0.616-2.011)	0.722
Node-pos	110	1.039 (0.504-2.141)	0.918	1.111 (0.646-1.911)	0.703	0.703 (0.503-0.984)	0.040

Abbreviations: HR, hazard ratio; 95% CI, confidence interval.

Western blotting. These experiments show that the expression of ADAM-15A and ADAM-15B isoforms may affect the spatial organization of focal adhesions and the cytoskeleton, which could affect the adhesion and migration behavior of the cells.

Cell Adhesion, Migration, Invasion, and Metastasis of ADAM-15 Stably Transfected MDA-MB-435 Cells

We carried out adhesion and migration assays to evaluate the effects of ADAM-15 isoform expression (Fig. 5). The ADAM-15A–transfected cells attached to tissue culture plastic more

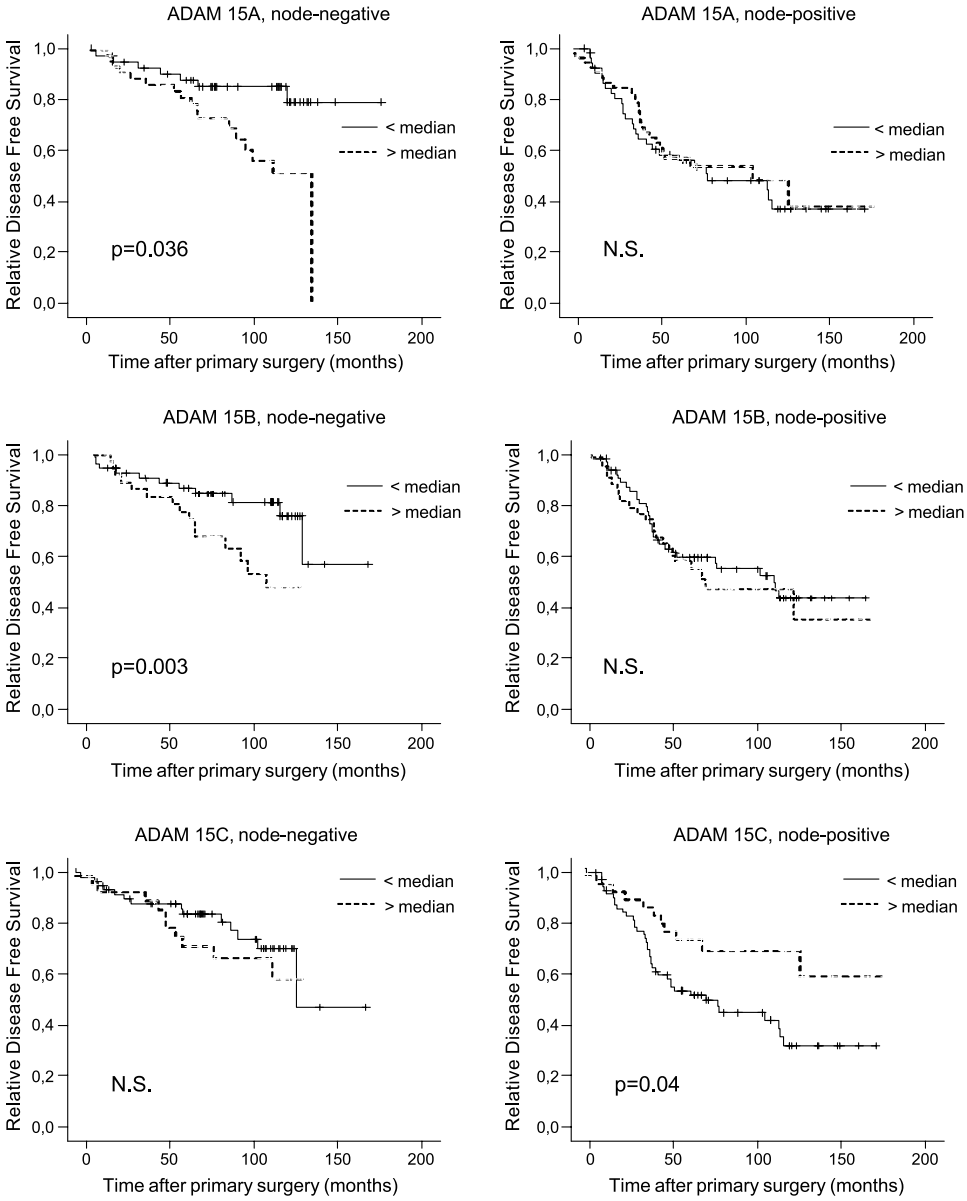

FIGURE 3. Relationships between ADAM-15 isoform expression and survival in node-negative and node-positive breast cancer patients. Expression of ADAM-15A, ADAM-15B, and ADAM-15C mRNAs were quantified in a second independent cohort of 229 breast cancer patients, and correlated with clinical outcome. Patients were divided into high (>median) and low (<median) levels of the individual ADAM isoforms. Continuous line, low-level expression; dotted line, high-level expression. *X* axis, time after surgery in months; *Y* axis, relapse-free survival in percent (see Materials and Methods).

Downloaded from mcr.aacrjournals.org on September 22, 2021. © 2008 American Association for Cancer Research.

Published OnlineFirst February 22, 2008; DOI: 10.1158/1541-7786.MCR-07-2028

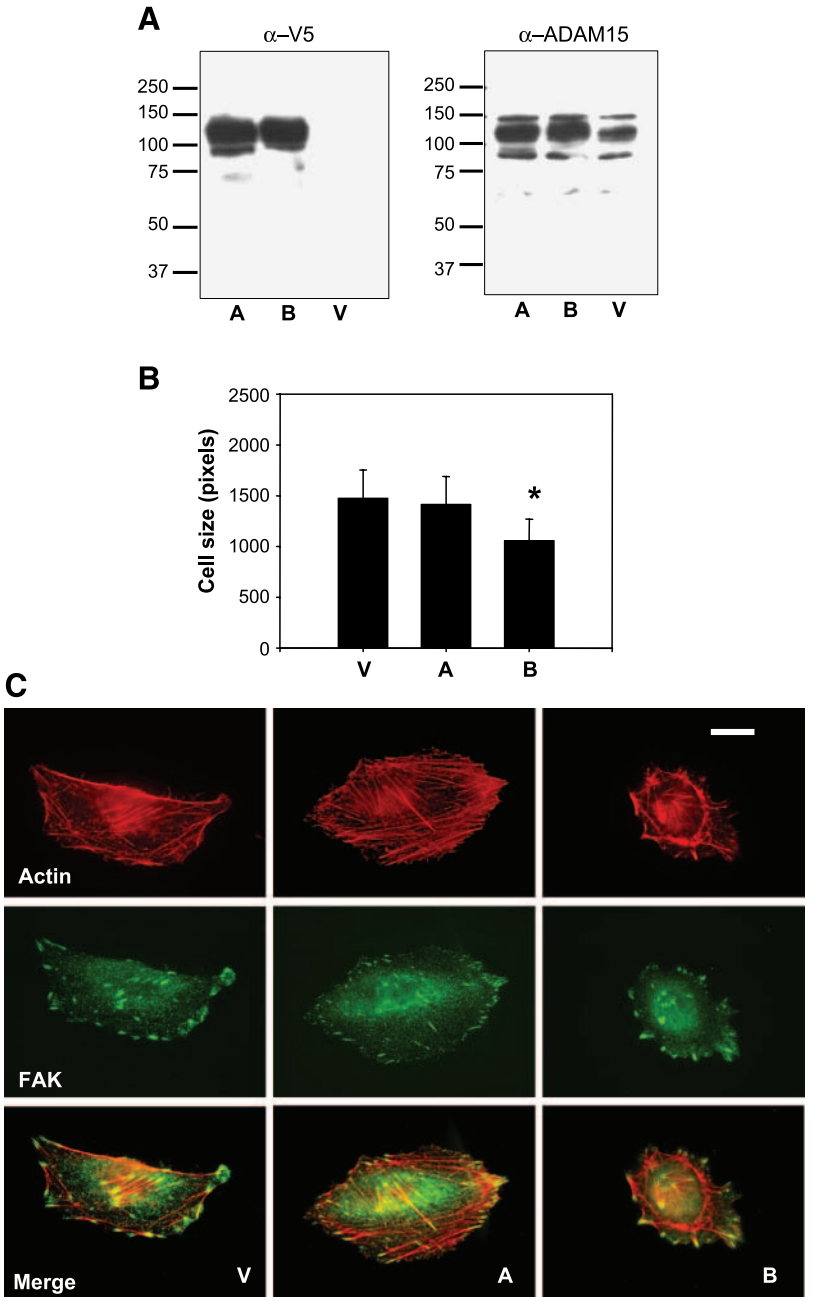

FIGURE 4. Characterization of ADAM-15 stably transfected MDA-MB-435 cells. **A.** Western blot analysis: Cell lysates were blotted with antibodies to the V5 epitope tag and to ADAM-15 as indicated. Representative clones of *ADAM15A* and *ADAM15B* that displayed equivalent levels of tagged protein were used for further studies. **B.** Cell size was determined by counting pixels in the images of 15 to 20 cells in fields chosen at random. **C.** Immunocytochemical analysis of FAK localization and morphology of the actin cytoskeleton. F-actin (*top*) was stained with rhodamine-phalloidin; FAK immunostaining (*middle*) was carried out as described in Materials and Methods. The merged image of FAK and actin staining is shown in the bottom panel. Scale bar, 20 μm.

effectively than either ADAM-15B or vector control cells ($P < 0.05$). The ADAM-15B–expressing cells exhibited significantly less attachment compared with the vector control cells ($P < 0.01$). Hence, the adhesion followed a decreasing order of ADAM-15A > vector > ADAM-15B. The same result was obtained when cells were allowed to adhere to dishes coated with fibronectin or laminin, suggesting that this was not related to increased ability to bind to a specific matrix component (data not shown). In parallel, we also carried out de-adhesion assays (Fig. 5B), whereby growing cultures of each cell type were washed and incubated in EDTA-EGTA, and the proportion of cells remaining attached were quantified. This assay showed that ADAM-15B–expressing cells detached more easily than vector control or ADAM-15A transfectants, revealing the same order of adhesive properties of the cells transfected with the ADAM-15 variants as the adhesion assay. A similar pattern of decreased adhesion of ADAM-15B–transfected cells was seen in a second breast cancer cell line, MCF-7 (Fig. 5C). Thus, ADAM-15B–expressing cells are considerably less adherent than vector control–transfected or ADAM-15A–expressing cells.

We also evaluated the migratory behavior of cells grown as a confluent monolayer and subjected to a scratch wound (Fig. 5D). The ADAM-15A cells migrated into the wound site more quickly than either vector control or ADAM-15B cells, which behaved quantitatively similarly in this assay. In parallel, Matrigel invasion assays (Fig. 5E) reflected a similar pattern to

Downloaded from mcr.aacrjournals.org on September 22, 2021. © 2008 American Association for Cancer Research.

Published OnlineFirst February 22, 2008; DOI: 10.1158/1541-7786.MCR-07-2028

the scratch wound assay, with ADAM-15A–transfected cells again showing the greatest invasive ability. However, in tail vein experimental metastasis assays, both the ADAM-15A and ADAM-15B clones showed reduced lung colonization ability compared with vector-transfected MDA-MB-435 cells (Fig. 5F; $P = 0.004$; $P = 0.022$, respectively). However, the ADAM-15B transfectants gave more lung foci than their ADAM-15A counterparts ($P = 0.035$).

ADAM-15 Cytoplasmic Domains Display Isoform-Specific Association with Intracellular Signaling Effectors

We have shown previously that the cytoplasmic tail of ADAM-15A associates with Src family protein tyrosine kinases and the adaptor protein Grb2 (18). We used the same approach of glutathione *S*-transferase (GST) pull-down assay to analyze the spectrum of proteins in extracts from MDA-MB-435 cells that could interact with the cytoplasmic domains of ADAM-15A, ADAM-15B, and ADAM-15C. Figure 6 shows that all the ADAM-15 isoforms were able to interact with Grb2 to similar extents. We also saw equal binding to the adaptor protein Tks5/Fish, which has been reported by Abram (17) to bind via its SH3 domain with ADAM-15. Interestingly, all three forms of ADAM-15 also interacted with ERK1/2 (Fig. 6) and P-ERK1/2 (data not shown). However, striking differences were observed in the association of ADAM-15 cytoplasmic tails with the adaptor protein Nck and the Src protein tyrosine

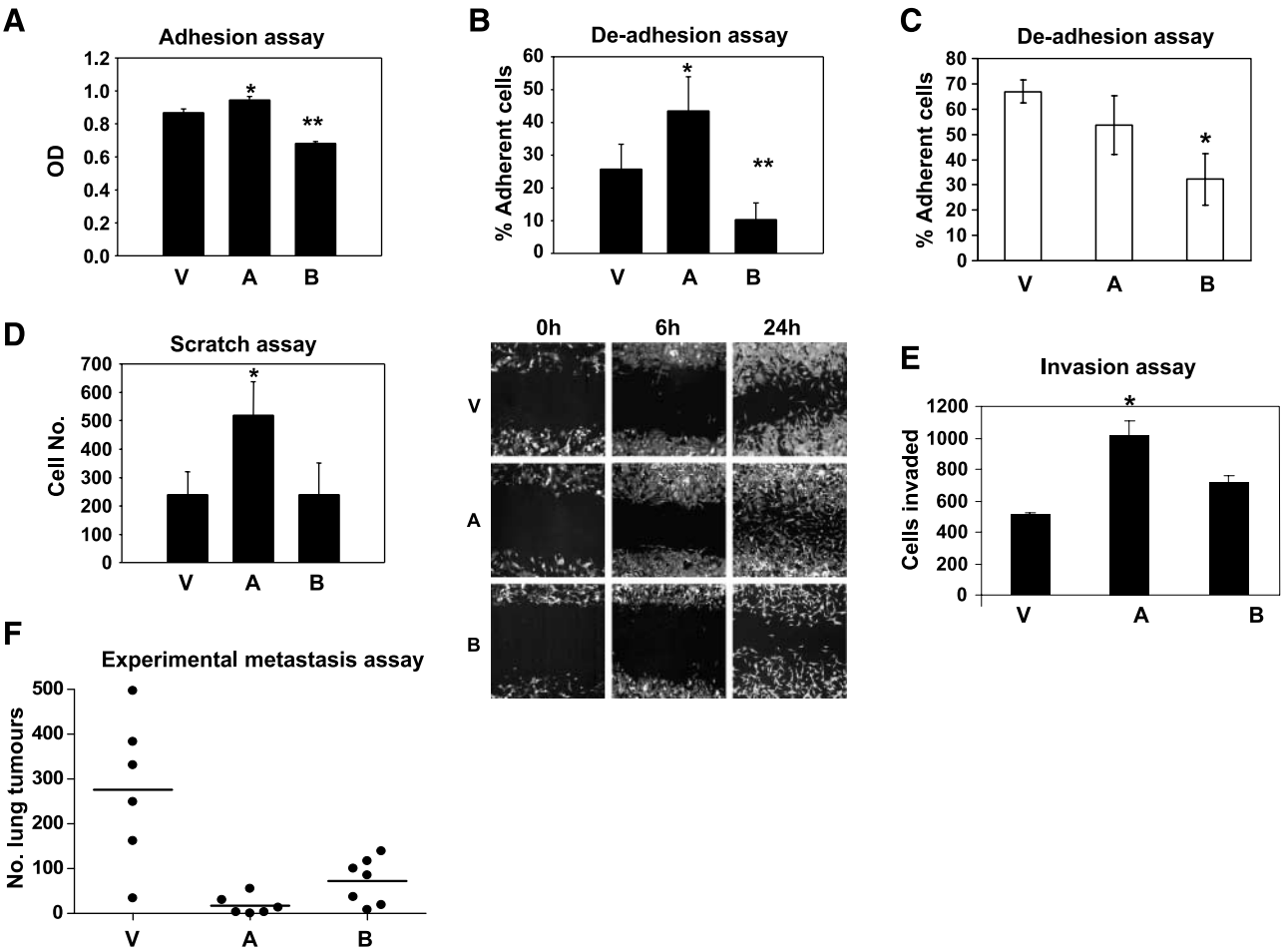

FIGURE 5. Cell adhesion, migration, invasion, and metastasis of ADAM-15 stably transfected cells. **A.** Cell adhesion: 8×10^4 MDA-MB-435 cells were seeded in triplicate in 96-well plates in serum-free medium and incubated for 1 h at 37°C, and then washed well with warm PBS, fixed, and stained with methylene blue; their absorbance was determined at 630 nm. Each clone was tested in triplicate (*V,* vector control; *A,* ADAM-15A; *B,* ADAM-15B). Columns, mean of three independent experiments; bars, SD. **B.** De-adhesion assay: Growing MDA-MB-435 cells were washed and incubated either in PBS or with EDTA-EGTA for 5 min as in Materials and Methods. The percentage of cells remaining attached were determined as for the adhesion assay (data are the SE values of two clones). **C.** De-adhesion assay with stably transfected MCF-7 cells: Cells were treated as in **B** either in PBS or with EDTA-EGTA for 5 min. The percentage of cells remaining attached were determined as for the adhesion assay (data are the SE values of two independent experiments with one clone of each type assayed in triplicate in each experiment.). **D.** Scratch wound assay: Confluent MDA-MB-435 cells in chamber slides were wounded by scratching using micropipette tips and were incubated with 2% FCS medium for 24 h. Cells migrating into the wound side were counted and data from three experiments were plotted (*left*); wound closure was also shown (*right*). Significance was determined by the *t* test (*$P < 0.05$, **$P < 0.01$). **E.** Matrigel invasion of MDA-MB-435 cells overexpressing ADAM-15 variants. Overexpression of variant A led to a significant induction (99%, $P = 0.029$) of Matrigel invasion, whereas there was no significant difference between the other groups (mean ± SE, *V*: 467.3 ± 55.4, $n = 4$; *A*: 931.3 ± 173.9, $n = 4$; *B*: 658.5 ± 96.7, $n = 4$). **F.** Experimental metastasis assay. Significant reduction of the number of X-gal–stained lung colonies by overexpression of ADAM-15A and ADAM-15B variants in MDA-MB-435 cells compared with the vector-transfected control group (*V* versus *A,* $P = 0.022$; *V* versus *B,* $P = 0.004$). Dots, result of one mouse; bar, mean (*V*: 276 ± 67.23 SE, $n = 6$; *A*: 17.33 ± 8.77, $n = 6$; *B*: 72.14 ± 19.27, $n = 7$).

Downloaded from mcr.aacrjournals.org on September 22, 2021. © 2008 American Association for Cancer Research.

Published OnlineFirst February 22, 2008; DOI: 10.1158/1541-7786.MCR-07-2028

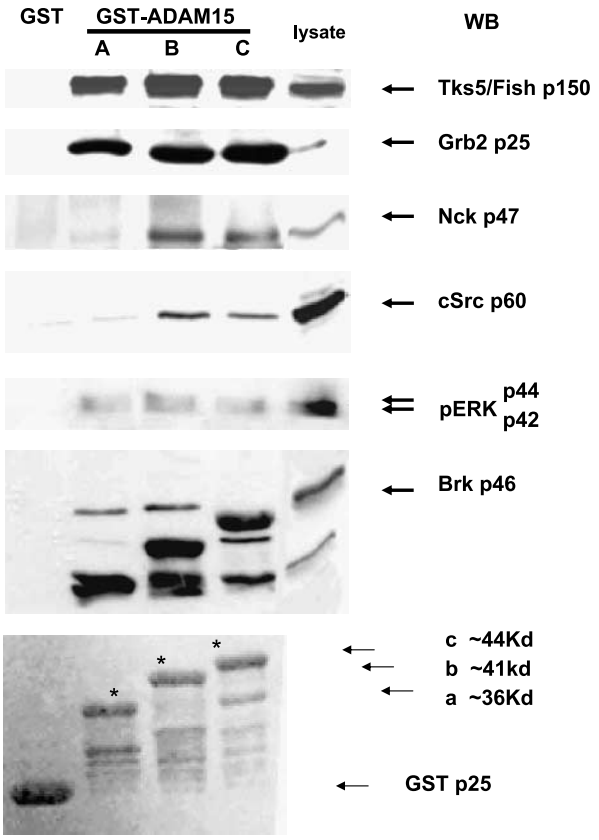

FIGURE 6. ADAM-15 cytoplasmic tail variants selectively associate with signaling molecules. GST-ADAM-15 cytoplasmic domain fusion proteins (ADAM-15A, ADAM-15B, and ADAM-15C) and GST control were used for pull-down assays with lysate from MDA-MB-435 cells (lysate alone shown in the *right-hand lane*). Bound proteins were separated by SDS-PAGE and transferred to polyvinylidene difluoride membranes, followed by Western blotting (*WB*) using the indicated antibodies. Bottom, Coomassie blue stain for GST fusion protein demonstrating equal loading of the proteins. *, the GST–ADAM-15 tail proteins.

kinase. Both proteins interacted efficiently with ADAM-15B and ADAM-15C but binding was much weaker (although still detectable above the background of GST alone) with ADAM-15A. In contrast, Brk (breast tumor tyrosine kinase) failed to bind to ADAM-15C (the lower bands in the blot in Fig. 5 are attributable to cross-reactivity with the GST fusion proteins, migration of which is shown in the bottom panel). Brk showed strong binding to ADAM-15A and ADAM-15B. Thus, these data show that the ADAM-15 variant cytoplasmic domains associate with distinct repertoires of intracellular signaling effectors in MDA-MB-435 cancer cells.

Discussion

The present work has revealed differential expression in human breast cancers of isoforms of ADAM-15 that differ only in the sequences of their cytoplasmic domain. Expression of two isoforms (ADAM-15A and ADAM-15B) was associated with a worse outcome in patients with node-negative disease, whereas a second isoform (ADAM-15C) was linked with improved relapse-free survival in patients with node-positive disease. The full-length ADAM-15A and ADAM-15B isoforms had differential effects on cancer cell shape, adhesion, migration, invasion, and metastatic ability and also the alternative cytoplasmic domains associated with different combinations of proteins involved in signal transduction. We suggest that the ADAM-15 variants may exert their effects by acting as platforms for assembly of distinct signaling complexes, and therefore that overexpression of specific isoforms may have consequences for processes associated with tumor growth, invasion, and metastasis.

Our expression studies showed that at the mRNA level, total ADAM-15 expression did not vary between normal mammary glands and tumor tissues, which is supported by data reported by Lendeckel et al. (34). However, one recent study has shown elevated expression of ADAM-15 RNA and protein in breast and prostate cancer (26). It is clear from our data that individual splice variants of ADAM-15 show distinct patterns of expression, with ADAM-15B and ADAM-15C isoforms being selectively increased in breast cancer compared with normal tissues, whereas the ADAM-15A and ADAM-15D variants were unaltered. These data concur with the analysis of Ortiz et al. (25) who found no major variation in total ADAM-15 RNA levels between normal mammary epithelial cells and a panel of 25 breast cancer cell lines, despite frequent changes in gene copy number. These authors concluded that nonmalignant cells predominantly expressed the isoform we identify as ADAM-15A, and the breast cancer cell lines showed increased levels of the more complex variants. Given that there are 23 exons in *ADAM15*, the patterns of alternative splicing that we and others have observed are nonrandom because only the cytoplasmic domain is affected, and therefore unlikely to be attributable to a general defect in splicing control in cancer cells (35), but instead suggests that there is functional relevance to such a complex and highly regulated pattern of exon usage.

We undertook functional analysis by contrasting the effects of overexpression in MDA-MB-435 cells of the ADAM-15A and ADAM-15B variants, observing that ADAM-15A did not significantly alter cell morphology, yet it promoted cell adhesion, migration, and invasion. In contrast, ADAM-15B–expressing cells appeared smaller (i.e., less well spread), with fewer focal adhesions, and with less filamentous actin. This isoform also decreased cell attachment, which may contribute to the lower Matrigel invasion capabilities of ADAM-15B–expressing cells compared with the ADAM-15A cells. There is substantial evidence that ADAM-15 can influence both cell adhesion and migration (31, 36, 37). Interactions of ADAM-15 disintegrin domain with integrins $\alpha_v\beta_3$, $\alpha_5\beta_1$, and $\alpha_9\beta_1$ have been documented (5-7), and these may in principle occur either *in trans*, regulating cell-cell adhesion, or *in cis*, thereby modulating cell interactions with matrix substrata. Overexpression of ADAM-15 (this is likely the originally described ADAM-15A variant) in NIH 3T3 cells enhanced cell attachment and led to increased cell-cell adhesion, with a concomitant decrease in migration (37). We did not observe increased cell-to-cell interactions in our MDA-MB-435–transfected clones, but this may depend on the spectrum of adhesive proteins that particular cell types express. Homotypic adhesion of human T lymphocytes, and their heterotypic adhesion to CaCo-2 intestinal epithelial cells, has recently been shown to be enhanced by ADAM-15 and to involve the RGD

Downloaded from mcr.aacrjournals.org on September 22, 2021. © 2008 American Association for Cancer Research.

Published OnlineFirst February 22, 2008; DOI: 10.1158/1541-7786.MCR-07-2028

motif in the disintegrin domain (38). In endothelial cells, ADAM-15 was found to localize with VE-cadherin at adherens junctions, and coexpression of VE-cadherin and ADAM-15 in Chinese hamster ovary cells resulted in their colocalization (39). This argues that the particular outcome of ADAM-15 expression may depend not only on the isoform that is overexpressed but also on the nature of other cell surface adhesive proteins. In $\alpha_v\beta_3$-expressing OV-MZ-6 ovarian cancer cells, overexpression of ADAM-15 (although it is unclear which isoform was expressed) led to reduction of $\alpha_v\beta_3$-mediated adhesion to vitronectin, along with decreased random cell motility (22). These data resemble in part our observations with ADAM-15B–transfected MDA-MB-435 cells. However, we have no evidence for modulation by ADAM-15 of specific matrix adhesive interactions; rather, the same pattern of altered adhesion was apparent on plastic, fibronectin, and laminin. This suggests that the effects of the different cytoplasmic domains of ADAM-15A and ADAM-15B may be more relevant than the interactions mediated by their common extracellular domains. This is borne out by the work of Charrier et al. (38) on T-lymphocyte–epithelial cell interactions, which required the ADAM-15 cytoplasmic domain.

Data from the clinical specimens showed that elevated ADAM-15A and ADAM-15B expression levels correlated with poorer survival in node-negative patients. This argues that the ADAM-15 status affects events at the site of the primary tumor, with these ADAM-15 isoforms potentially promoting dissemination from the primary site; however, once metastases have occurred, their role is less significant. This may have bearing on the *in vivo* experimental metastasis assay, which showed that cells expressing either isoform showed less lung colonization ability compared with vector controls. However, the ADAM-15B–expressing cells generated more metastatic foci than the A transfectants, again consistent with differential effects on cell behavior. The association of ADAM-15C expression with enhanced survival in node-positive patients suggests that this isoform may influence the growth of metastases, or perhaps responses to the adjuvant chemotherapy that patients subsequently received. Given the involvement of ADAM-15 in lymphocyte-epithelial cell interactions (38), enhanced immune surveillance in ADAM-15C–expressing tumors is an attractive possibility. Taken together, these findings suggest that the effects of the ADAM-15 isoforms on mammary cancer development are complex, potentially affecting the tumor microenvironment at either the site of origin or in metastatic foci, and may not be modeled effectively by simplified invasion and metastasis assays.

We and others have shown previously that the ADAM-15 cytoplasmic domains are capable of associating with diverse SH3- and SH2-domain containing proteins, including Grb2, MAD2, endophilin, Tks5/Fish, and Src family protein-tyrosine kinases (17, 18, 31, 40). These associations, plus others with additional SH3 domain proteins, have recently been confirmed in a phage display analysis (41). Using pull-down analysis with GST-ADAM-15 cytoplasmic domain fusion proteins, we showed that ADAM-15A and ADAM-15B were essentially equally effective in interacting with the adaptor proteins Grb2 and Tks5/Fish, with the breast tumor tyrosine kinase Brk (42), and with ERK and P-ERK. However, differences were clearly apparent for the interaction with Src and with the adaptor protein Nck, which were bound more effectively by ADAM-15B. Yasui et al. (40) have also reported similar findings for the preferential interaction of ADAM-15C (in their terminology, ADAM15v2) with the Src family protein tyrosine kinases Lck and Hck compared with ADAM-15A (ADAM15v). At present, the molecular basis for these interactions are unknown but mutational studies with ADAM-15A have shown that Grb2 binding involves the COOH-terminal portion of the cytoplasmic domain, whereas Lck interaction involved the membrane-proximal part (18). Inclusion of the additional proline-rich motifs in ADAM-15B might significantly alter the protein topology generating the observed selectivity. It is interesting that ADAM-15B was able to interact effectively with all of the proteins examined, whereas ADAM-15A and ADAM-15C showed greater selectivity. This may provide some insight into the association of ADAM-15B overexpression with worse outcome in breast cancer patients: This protein may create a binding platform that brings into proximity a particular cast of signaling molecules that can trigger pathways that alter cellular interactions with the extracellular environment, promoting cell detachment and ultimately metastatic spread. Other ADAM-15 variants may omit key participants from these signaling assemblies, leading to less aggressive patterns of cell behavior. Alternatively, it is possible that overexpression of the ADAM-15 proteins causes sequestration of signaling proteins away from bona fide signaling receptors (e.g., growth factor receptors and integrins), potentially influencing the balance between activation and inhibition of downstream pathways.

ADAM15 is localized to chromosome 1q 21.3, which is a region that is amplified in several types of cancers including breast cancer (28, 43). The ADAM-15 protein is involved in angiogenesis, because *Adam15*$^{-/-}$ mice show reduced tumor angiogenesis, and recombinant ADAM-15 disintegrin domain containing the RGD sequence inhibits angiogenesis, tumor growth, and metastasis (44). However, in breast tumors, ADAM-15 is localized primarily to the tumor cells themselves (26), indicating that its major actions are probably exerted on the cancer cell itself, potentially via modulation of integrin-mediated cell adhesion or its proteolytic activity, such as its ability to transactivate the epidermal growth factor receptor by processing heparin-binding epidermal growth factor (8, 45). Our analysis provides functional evidence for a role of variant ADAM-15 cytoplasmic tails in modulating cell adhesion and migration via their abilities to interact with different intracellular signaling effectors. Important future questions are whether the effects of the ADAM-15 variants require the engagement of their extracellular disintegrin and metalloproteinase functions, and the nature of the protein interactions that are responsible for the specific ability of ADAM-15B isoforms to regulate malignancy.

Materials and Methods

Tissue Samples, RNA Isolation, Reverse Transcription, and Quantitative Real-time PCR

An initial survey of mammary tumor and normal tissue (32) involved 48 human invasive breast carcinomas obtained from the human tissue bank at the Norfolk and Norwich University

Downloaded from mcr.aacrjournals.org on September 22, 2021. © 2008 American Association for Cancer Research.

Published OnlineFirst February 22, 2008; DOI: 10.1158/1541-7786.MCR-07-2028

Hospital and 10 nonneoplastic human mammary tissue samples obtained from patients at reduction mammoplasty. The study received the approval of the Norwich District Ethical Committee (LREC 98/037) and the Norfolk Research Ethics Committee (05/Q0101/202), and the East Norfolk and Waveney Research Governance Committee. A further 229 human primary breast tumor samples were obtained from the human tissue bank of the Department of Chemical Endocrinology of the Radboud University Nijmegen Medical Centre, Nijmegen, the Netherlands. Coded tumor tissues were used in accordance with the Code of Conduct of the Federation of Medical Scientific Societies in the Netherlands ("Code for Proper Secondary Use of Human Tissue in the Netherlands"[5]) and this study adhered to all relevant institutional and national guidelines. Total RNA was isolated using 20 mg of tissue powder obtained by microdismembration in liquid nitrogen with the RNeasy mini kit (Qiagen) with on-column DNase-I treatment as described earlier (33). Subsequent reverse transcription and TaqMan PCR procedures were as described previously (32, 46). *ADAM15* isoform–specific primers and minor groove-binding probes were made by Applied Biosystems. The following sequences were used: *ADAM15A*: forward 5′-CAGGACCTCCGCAGAG-3′, reverse 5′-GCAGGCAGTGGCTTCCTT-3′, probe 5′-ACGAGGCACTAAGTCTCA-3′; *ADAM15B*: forward 5′-GCCTGACCCTGTGTCCAA-3′, reverse 5′-GCAGGCAGTGGCTTCCTT-3′; probe 5′-CCCCTGAGACTGGAGTCT-3′; *ADAM15C*: forward 5′-CTGACCCGGTGGTGAGAAG-3′, reverse 5′-GCAGGCAGTGGCTTCCTT-3′, probe 5′-CCCCTGAGACTTCG-3′; *ADAM15D*: forward 5′-GCGACTCTGCCAGCTCAA-3′, reverse 5′-GCAGGCAGTGGCTTCCTT-3′, probe 5′-CTGCCAGTACAGTCTCAG-3′.

Antibodies

Anti-*ADAM15* antibodies were from Chemicon International; anti-Brk, anti-Tks5/Fish, and anti-Grb2 were obtained from Santa Cruz Biotechnology; anti-phosphotyrosine (PY), anti-vinculin, anti-FAK, and anti-Src were all purchased from Upstate Biotechnology; anti-ERK was from Cell Signaling Technology; anti-V5 was from Invitrogen; and anti-Nck was from Stratech Scientific, Ltd. Secondary antibodies, anti-rat, anti-rabbit, and anti-mouse/horseradish peroxidase were from Vector Laboratories.

Construction of Full-length ADAM15 Expression Vectors

The full-length *ADAM15A* was cut from the parental pcDNA3 (18) with *Hin*dIII and was gel eluted. To generate isoform-specific cDNA and to delete the stop codon, the *Hin*dIII DNA fragment was cut with *Bss*SI (which cuts in the cytoplasmic domain close to the membrane-spanning region) and ligated with PCR amplified *Bss*SI-*Xho*I cytoplasmic domain isoforms obtained by reverse transcription-PCR from human breast tumor RNA, followed by ligation into pcDNA4-V5-His vector cut with *Hin*dIII and *Xho*I. The resulting plasmids have the full-length ADAM-15 with ADAM-15A, ADAM-15B, or ADAM-15C cytoplasmic domains, followed by V5 and His epitopes. For generation of stably transfected clones, the expression vectors were linearized by digestion with *Sca*I (which cuts in the ampicillin resistance locus, outside the Zeocin resistance, and *ADAM15* expression cassettes).

Cell Culture

MDA-MD-435 cells were maintained in DMEM supplemented with 10% heat-inactivated FCS, L-glutamine, and antibiotics. MCF7 cells were maintained in Earle's MEM supplemented with 10% heat-inactivated FCS, L-glutamine, sodium pyruvate, nonessential amino acids, and antibiotics. Cells were transfected with linearized expression plasmids using Fugene 6 (Roche Diagnostics, Ltd). Two weeks after Zeocin selection (200 μg/mL), emerging resistant colonies were picked using cloning rings and expanded. Cells stably expressing *ADAM15* isoforms were maintained in DMEM, supplemented with 10% heat-inactivated FCS, L-glutamine, antibiotics, and Zeocin.

GST-ADAM15 Cytoplasmic Domain Fusion Proteins

ADAM15 cytoplasmic domain isoforms were amplified from breast tumor samples by reverse transcription-PCR. The amplified products were cloned into pGEX-5X-1 in-frame with GST as described (18). Production and purification of the GST fusion proteins were done as described previously (18).

Pull-Down Assays

Pull-down assays with GST fusion proteins were done as described (18). Briefly, monolayers of MDA-MB-435 cells were grown to confluency and lysed on ice in NP40 lysis buffer [50 mmol/L Tris-HCl (pH7.5), 150 mmol/L NaCl, 1.5 mmol/L $MgCl_2$, 10% glycerol, and 1% NP40] supplemented with proteinase and phosphatase inhibitors, then scraped into Eppendorf tubes, cleared from cell debris by centrifugation, and quantified. GST fusion protein/Sepharose slurry (2-4 μg) was added to protein lysate from $\sim 5 \times 10^5$ cells. After 1-h incubation at 4°C on a rotator, beads were washed thrice with the same lysis buffer, resolved on SDS-PAGE, and subjected to immunoblotting.

Western Blotting

Cell lysates prepared as for pull-down assays were centrifuged at 13,000 × *g* for 20 min at 4°C, and the supernatants were collected and protein concentrations were determined by BCA assay (Bio-Rad). Ten micrograms of protein were separated on 7.5% or 10% (w/v) SDS-PAGE and transferred to polyvinylidene difluoride (Millipore) membranes and blotted with the indicated antibodies according to standard methods. Appropriate horseradish peroxidase–conjugated secondary antibodies were added and immunoreactive proteins were detected on films, visualized by the enhanced chemiluminescence Western blot detection system (Amersham Biosciences).

De-Adhesion Assay

Cells were seeded in triplicate in 96-well (MDA-MB-435) or 24-well plates (MCF-7) in DMEM supplemented with 10% FCS. At 72 h, medium was changed to serum-free medium and

[5] http://www.fmwv.nl

Downloaded from mcr.aacrjournals.org on September 22, 2021. © 2008 American Association for Cancer Research.

Published OnlineFirst February 22, 2008; DOI: 10.1158/1541-7786.MCR-07-2028

the cells were allowed to incubate overnight. After the cells had been washed in PBS, 1 mmol/L EDTA-EGTA was added and cells were further incubated for 5 min. Then, the EDTA-EGTA was decanted and the cells were washed and fixed in 95% ethanol. Excess liquid was removed at 1 h and cells were stained with methylene blue. Cells were washed thoroughly with water, the color was extracted with 50% ethanol–0.1 mol/L HCl, and absorbance was read at 630 nm.

Cell Adhesion Assay

Cells (8×10^4) were seeded in triplicate in 96-well plates in serum-free medium and incubated for 1 h at 37°C and 5% CO_2. Medium was decanted off and the attached cells were washed well with warm PBS and then fixed, and absorbance was read at 630 nm as described above.

Scratch Assay (Wound Healing Assay) and Time Course of Scratch Assay

Cells (5×10^4) were seeded in triplicate in a 24-well plate in DMEM supplemented with 10% FCS and incubated at 37°C for 48 h until confluent, and the monolayers were then wounded by scratching with the 200 μL tip of a yellow pipette. Cells were washed and fresh DMEM containing 2% FCS was added and the plates were incubated for up to 24 h. Following wounding, an image was taken at time 0 using the Lucia 32G/Magic 4.11 computer software system (Nikon) and at 24 h after wounding. Migration was measured by counting the number of cells that migrated into the wound in three random fields per triplicate sample. In some experiments, cells were seeded in chamber slides (BD Bioscience) until confluent, wounded as described, and subsequently immunostained with the indicated antibodies.

Invasion Assay

MDA-MD-435 cells or the respective *ADAM15*-transfected clones (1×10^5) were seeded in FCS-free medium in the upper compartment of Matrigel (BD Biosciences)–coated Boyden chambers (Costar) in triplicates. Boyden chambers were placed in plates containing 10% FCS–supplemented medium. Invaded cells were counted after 48 h after staining with a Quick-Diff Staining kit (DADE Behring).

Experimental Metastasis Assay

Pathogen-free, athymic $CD1^{nu/nu}$ mice (Charles River) were injected i.v. with 5×10^5 *lacZ*-tagged MDA-MD-435 cells or the respective *ADAM15*-transfected clones. Forty-two days after inoculation, mice were sacrificed and lungs were removed. Lungs were stained with X-gal (5-bromo-4-chloro-3-indolyl-β-D-galactopyranoside, Roche Diagnostics) as described (47). Blue macrometastatic foci on the surface of the lungs were counted. All animal experiments were done in compliance with the guidelines of the Tierschutzgesetz des Landes Oberbayern.

Immunostaining and Immunofluorescence

MDA-MB-435 cells and *ADAM15* stably transfected clones were cultured on heat-sterilized coverslips, then washed in PBS, fixed in 4% (w/v) paraformaldehyde for 15 min, and permeabilized with 0.1% Triton for 10 min. Cells were washed well with PBS and blocked with 10% goat serum or 8% bovine serum albumin (for the anti-vinculin antibody). Primary antibodies such as mouse or rabbit anti-V5 antibody (1:1,000), mouse anti-vinculin (1:100), and anti-4G10 (1:1,000) were added for 1 h. After repeated washes in PBS, Alexa-488–conjugated goat-anti mouse/rabbit IgG, or Alexa-568–conjugated goat-anti mouse/rabbit IgG (both 1:1,000 dilution, Molecular Probes), was applied for 30 min. For detection of actin filament, rhodamine-conjugated phalloidin (1:150, Molecular Probes) was used. After washing, the coverslips were mounted with Hydromount (National Diagnostics). Controls involved omission of the primary antibody and use of an irrelevant control IgG. Fluorescence was visualized by using a Zeiss epifluorescence microscope (Germany) at 488 nm (FITC) and 568 nm (rhodamine). Images were taken using AxionVision 4. Images were examined with ×50, ×200, and ×630 magnification and then edited using Photoshop 6.

Statistical Analyses

Statistical analyses were carried out using SPSS 12.0.1 software (SPSS Benelux BV). Normality of distribution was tested by the method of Kolmogorov-Smirnov. Differences in the proportion of tumors with more or less than the median level of expression of each *ADAM15* isoform from patients categorized by clinical-pathologic characteristics, used as grouping variables, were assessed with Pearson χ^2 test or Spearman correlation if more than two ordinal categories were involved. As data on histologic grading were missing for a substantial number of patients, this group was included in all analyses as a separate group. Relapse-free survival time, defined as the time from surgery until diagnosis of recurrent disease, was used as follow-up end point. The Cox proportional hazards model was used to assess the prognostic value of *ADAM15* expression as entered as a continuous variable. For visualization purposes, survival curves were generated using the method of Kaplan and Meier after dichotomization of the patients based on the median expression levels of *ADAM15* isoforms. Equality of survival distributions was tested using log-rank testing. Two-sided *P* values below 0.05 were considered to be statistically significant (32).

References

1. Schlondorff J, Blobel CP. Metalloprotease-disintegrins: modular proteins capable of promoting cell-cell interactions and triggering signals by protein-ectodomain shedding. J Cell Sci 1999;112:3603–17.

2. Blobel CP. ADAMs: key components in EGFR signalling and development. Nat Rev Mol Cell Biol 2005;6:32–43.

3. Black RA, White JM. ADAMs: focus on the protease domain. Curr Opin Cell Biol 1998;10:654–9.

4. Krätzschmar J, Lum L, Blobel CP. Metargidin, a membrane anchored metalloprotease-disintegrin protein with an RGD integrin binding sequence. J Biol Chem 1996;271:4593–6.

5. Nath D, Slocombe PM, Stephens PE, et al. Interaction of metargidin (ADAM-15) with vβ3 and 5β1 integrins on different haemopoietic cells. J Cell Sci 1999; 112:579–87.

6. Zhang XP, Kamata T, Yokoyama K, Puzon-McLaughlin W, Takada Y. Specific interaction of the recombinant disintegrin-like domain of MDC-15 (metargidin, ADAM-15) with integrin vβ3. J Biol Chem 1998;273:7345–50.

7. Eto K, Puzon-McLaughlin W, Sheppard D, Sehara-Fujisawa A, Zhang XP, Takada Y. RGD-independent binding of integrin 9β1 to the ADAM-12 and -15 disintegrin domains mediates cell-cell interaction. J Biol Chem 2000;275:34922–30.

Downloaded from mcr.aacrjournals.org on September 22, 2021. © 2008 American Association for Cancer Research.

Published OnlineFirst February 22, 2008; DOI: 10.1158/1541-7786.MCR-07-2028

8. Hart S, Fischer OM, Prenzel N, et al. GPCR-induced migration of breast carcinoma cells depends on both EGFR signal transactivation and EGFR-independent pathways. Biol Chem 2005;386:845–55.

9. Kveiborg M, Frohlich C, Albrechtsen R, et al. A role for ADAM12 in breast tumour progression and stromal cell apoptosis. Cancer Res 2005;65:4754–61.

10. Wildeboer D, Naus S, Amy Sang QX, Bartsch JW, Pagenstecher A. Metalloproteinase-disintegrin ADAM8 and ADAM9 are highly regulated in human primary brain tumour and their expression levels and activities are associated with invasiveness. J Neuropathol Exp Neurol 2006;65:516–27.

11. Duffy MJ, Lynn DJ, Lloyd AT, O'Shea CM. The ADAMs family of proteins: from basic studies to potential clinical applications. Thromb Haemost 2003;89:622–31.

12. Seals DF, Courtneidge SA. The ADAMs family of metalloproteases: multidomain proteins with multiple functions. Genes Dev 2003;17:7–30.

13. Suzuki A, Kadota N, Hara T, et al. Meltrin α cytoplasmic domain interacts with SH3 domains of Src and Grb2 and is phosphorylated by v-Src. Oncogene 2000;19:5842–50.

14. Kang Q, Cao Y, Zolkiewska A. Direct interaction between the cytoplasmic tail of ADAM 12 and the Src homology 3 domain of p85α activates phosphatidylinositol 3-kinase in C2C12 cells. J Biol Chem 2001;276:24466–72.

15. Nelson KK, Schlondorff J, Blobel CP. Evidence for an interaction of the metalloprotease-disintegrin tumour necrosis factor α convertase (TACE) with mitotic arrest deficient 2 (MAD2), and of the metalloprotease-disintegrin MDC9 with a novel MAD2-related protein, MAD2β. Biochem J 1999;343:673–80.

16. Howard L, Nelson KK, Maciewicz RA, Blobel CP. Interaction of the metalloprotease disintegrins MDC9 and MDC15 with two SH3 domain-containing proteins, endophilin I and SH3PX1. J Biol Chem 1999;274:31693–9.

17. Abram CL, Seals DF, Pass I, et al. The adaptor protein Fish associates with members of the ADAMs family and localizes to podosomes of Src-transformed cells. J Biol Chem 2003;278:16844–51.

18. Poghosyan Z, Robbins SM, Houslay MD, Webster A, Murphy G, Edwards DR. Phosphorylation-dependent interactions between ADAM15 cytoplasmic domain and Src family protein-tyrosine kinases. J Biol Chem 2002;277:4999–5007.

19. Horiuchi K, Weskamp G, Lum L, et al. Potential role for ADAM15 in pathological neovascularization in mice. Mol Cell Biol 2003;23:5614–24.

20. Bohm BB, Aigner T, Roy B, Brodie TA, Blobel CP, Burkhardt H. Homeostatic effects of the metalloproteinase disintegrin ADAM15 in degenerative cartilage remodeling. Arthritis Rheum 2005;52:1100–9.

21. Wu E, Croucher PI, McKie N. Expression of members of the novel membrane linked metalloproteinase family ADAM in cells derived from a range of haematological malignancies. Biochem Biophys Res Commun 1997;235:437–42.

22. Beck V, Herold H, Benge A, et al. ADAM15 decreases integrin αvβ3/vitronectin-mediated ovarian cancer cell adhesion and motility in an RGD-dependent fashion. Int J Biochem Cell Biol 2005;37:590–603.

23. Carl-McGrath S, Lendeckel U, Ebert M, Roessner A, Rocken C. The disintegrin-metalloproteinases ADAM9, ADAM12, and ADAM15 are upregulated in gastric cancer. Int J Oncol 2005;26:17–24.

24. Schütz A, Härtig W, Wobus M, Grosche J, Wittekind Ch, Aust G. Expression of ADAM15 in lung carcinomas. Virchows Arch 2005;446:421–9.

25. Ortiz RM, Kärkkäinen I, Huovila AP. Aberrant alternative exon use and increased copy number of human metalloprotease-disintegrin ADAM15 gene in breast cancer cells. Genes Chromosomes Cancer 2004;41:36–378.

26. Kuefer R, Day KC, Kleer CG, et al. ADAM15 disintegrin is associated with aggressive prostate and breast cancer disease. Neoplasia 2006;8:319–29.

27. Kärkkäinen I, Karhu R, Huovila AP. Assignment of the ADAM15 gene to human chromosome band 1q21.3 by *in situ* hybridization. Cytogenet Cell Genet 2000;88:206–7.

28. Waltz MR, Pandelidis SM, Pratt W, et al. A microsatellite within the MUC1 locus at 1q21 is altered in the neoplastic cells of breast cancer patients. Cancer Genet Cytogenet 1998;100:63–7.

29. Kleino I, Ortiz RM, Huovila A-PJ. ADAM15 gene structure and differential alternative exon use in human tissue. BMC Mol Biol 8:90.

30. Charrier L, Yan Y, Driss A, Laboisse CL, Sitaraman SV, Merlin D. ADAM-15 inhibits wound healing in human intestinal epithelial cell monolayers. Am J Physiol Gastrointest Liver Physiol 2005;288:G346–53.

31. Shimizu E, Yasui A, Matsuura K, Hijiya N, Higuchi Y, Yamamoto S. Structure and expression of the murine ADAM 15 gene and its splice variants, and difference of interaction between their cytoplasmic domains and Src family proteins. Biochem Biophys Res Commun 2003;309:779–85.

32. Porter S, Span PN, Sweep FC, et al. ADAMTS8 and ADAMTS15 expression predicts survival in human breast carcinoma. Int J Cancer 2006;118:1241–7.

33. Span PN, Lindberg RL, Manders P, et al. Tissue inhibitors of metalloproteinase expression in human breast cancer: TIMP-3 is associated with adjuvant endocrine therapy success. J Pathol 2004;202:391–4.

34. Lendeckel U, Kohl J, Arndt M, Carl-McGrath S, Donat H, Rocken C. Increased expression of ADAM family members in human breast cancer and breast cancer cell lines. J Cancer Res Clin Oncol 2005;131,1:41–8.

35. Wang Z, Lo HS, Yang H, et al. Computational analysis and experimental validation of tumour-associated alternative RNA splicing in human cancer. Cancer Res 2003;63:655–7.

36. Martin J, Eynstone LV, Davies M, Williams JD, Steadman R. The role of ADAM15 in glomerular mesangial cell migration. J Biol Chem 2002;277:33683–9.

37. Herren B, Garton KJ, Coats S, Bowen-Pope DF, Ross R, Raines EW. ADAM15 overexpression in NIH3T3 cells enhances cell-cell interactions. Exp Cell Res 2001;271:152–60.

38. Charrier L, Yan Y, Nguyen HTT, et al. ADAM-15/metargidin mediates homotypic aggregation of human T lymphocytes and heterotypic interactions of T lymphocytes with intestinal epithelial cells. J Biol Chem 2007;282:16948–58.

39. Ham C, Levkau B, Raines EW, Herren B. ADAM15 is an adherens junction molecule whose surface expression can be driven by VE-cadherin. Exp Cell Res 2002;279:239–47.

40. Yasui A, Matsuura K, Shimizu E, Hijiya N, Higuchi Y, Yamamoto S. Expression of splice variants of the human ADAM15 gene and strong interaction between the cytoplasmic domain of one variant and Src family proteins Lck and Hck. Pathobiology 2004;71:185–92.

41. Kärkkäinen S, Hiipakka M, Wang JH, et al. Identification of preferred protein interactions by phage-display of the human Src homology-3 proteome. EMBO Rep 2006;7:186–91.

42. Harvey AJ, Crompton MR. Use of RNA interference to validate Brk as a novel therapeutic target in breast cancer: Brk promotes breast carcinoma cell proliferation. Oncogene 2003;22:5006–10.

43. Gendler SJ, Cohen EP, Craston A, Duhig T, Johnstone G, Barnes D. The locus of the polymorphic epithelial mucin (PEM) tumour antigen on chromosome 1q21 shows a high frequency of alteration in primary human breast tumours. Int J Cancer 1990;45:431–5.

44. Trochon-Joseph V, Martel-Renoir D, Mir LM, et al. Evidence of antiangiogenic and antimetastatic activities of the recombinant disintegrin domain of metargidin. Cancer Res 2004;64:2062–9.

45. Schäfer B, Marg B, Gschwind A, Ullrich A. Distinct ADAM metalloproteinases regulate G protein-coupled receptor-induced cell proliferation and survival. J Biol Chem 2004;279:47929–38.

46. Nuttall RK, Sampieri CL, Pennington CJ, Gill SE, Schultz GA, Edwards DR. Expression analysis of the entire MMP and TIMP gene families during mouse tissue development. FEBS Lett 2004;563:129–34.

47. Krüger A, Schirrmacher V, von Hoegen P. Scattered micrometastases visualized at the single-cell level: detection and re-isolation of lacZ-labeled metastasized lymphoma cells. Int J Cancer 1994;58:275–84.

Downloaded from mcr.aacrjournals.org on September 22, 2021. © 2008 American Association for Cancer Research.

Published OnlineFirst February 22, 2008; DOI: 10.1158/1541-7786.MCR-07-2028

AACR American Association for Cancer Research

Molecular Cancer Research

Distinct Functions of Natural ADAM-15 Cytoplasmic Domain Variants in Human Mammary Carcinoma

Julia L. Zhong, Zaruhi Poghosyan, Caroline J. Pennington, et al.

Mol Cancer Res 2008;6:383-394. Published OnlineFirst February 22, 2008.

Updated version Access the most recent version of this article at: doi:10.1158/1541-7786.MCR-07-2028

Cited articles This article cites 45 articles, 18 of which you can access for free at: http://mcr.aacrjournals.org/content/6/3/383.full#ref-list-1

Citing articles This article has been cited by 10 HighWire-hosted articles. Access the articles at: http://mcr.aacrjournals.org/content/6/3/383.full#related-urls

E-mail alerts Sign up to receive free email-alerts related to this article or journal.

Reprints and Subscriptions To order reprints of this article or to subscribe to the journal, contact the AACR Publications Department at pubs@aacr.org.

Permissions To request permission to re-use all or part of this article, use this link http://mcr.aacrjournals.org/content/6/3/383. Click on "Request Permissions" which will take you to the Copyright Clearance Center's (CCC) Rightslink site.

Downloaded from mcr.aacrjournals.org on September 22, 2021. © 2008 American Association for Cancer Research.